Linked-cluster expansion around the atomic limit of the Hubbard model

Walter Metzner*
Institut für Theoretische Physik C, Technische Hochschule Aachen, Sommerfeldstrasse 26/28, D-5100 Aachen, Federal Republic of Germany
(Received 4 October 1990)

We develop a perturbation expansion in the intersite hopping around the atomic limit of the Hubbard model. It is valid for arbitrary finite temperatures and interaction strengths. Diagrammatic rules that determine the grand-canonical potential and the Green's functions are derived. They reduce the calculation of any finite-order contribution to simple algebra. This opens the way for series extrapolations from computer-aided high-finite-order evaluations. Discrepancies in earlier expansions around the atomic limit are clarified. The present expansion scheme involves only *connected* diagrams with *unrestricted* lattice sums. This allows one to perform a vertex renormalization as for the linked-cluster expansion of the Ising model. The renormalized perturbation expansion can be used to construct self-consistent approximations which are automatically exact in the atomic limit. In the limit of high lattice dimensions, only fully two-particle reducible embeddings of diagrams on the lattice contribute. The single-particle properties of the infinite-dimensional Hubbard model reduce to those of *independent* tight-binding fermions hopping between dressed sites.

I. INTRODUCTION

A proper assessment of the correlation effects induced by strong, short-ranged interactions in Fermi systems is one of the most acute problems in today's condensed-matter theory. Even for the simplest models of strongly interacting fermions, exact solutions exist only in a few special cases, such as in one spatial dimension, while in general one is still disputing even the *qualitative* structure of the corresponding phase diagrams. The question about the existence of superconducting phases in lattice models of electrons with purely repulsive interactions, which has been intensively discussed in the context of high-T_c superconductivity,[1] is only the most spectacular among many other unsolved problems.

In the case of models with *localized* (spatially fixed) spins, such as Ising or Heisenberg models, much insight has been gained by expansions around the "atomic" limit, where intersite couplings are switched off.[2] In this approach one calculates the leading orders of an expansion for the thermodynamic potential, susceptibilities, etc., in powers of intersite coupling constants and tries to extrapolate the results to higher orders. In many situations this technique yields the most accurate quantitative estimates of critical exponents presently available.[3] In addition, renormalized series expansions have been used to construct self-consistent approximations that obey conservation laws and fundamental thermodynamic identities.[4]

In this work we develop a renormalized series expansion for the Hubbard model,[5-7] a lattice model of locally interacting *itinerant* fermions. The Hubbard model is one of the simplest models in the theory of correlated fermions where it plays a generic role similar to the Heisenberg or Ising model in the case of spin systems.

For interacting lattice fermions the method of series expansions around the atomic limit has not yet been systematically developed. For the Hubbard model, several static quantities such as the grand-canonical potential and some static susceptibilities have been expanded in powers of t_{ij}, where t_{ij} is the interatomic hopping amplitude (from site j to site i). The expansion has been carried out explicitly up to fourth order for general intra-atomic interaction strength U (Refs. 8–10) and up to ninth order for $U=\infty$.[11,12] The results have been used to study magnetic properties of the Hubbard model such as, in particular, the critical temperature for the onset of ferromagnetism in various lattice structures. However, different authors obtained different results and, consequently, arrived at contrasting conclusions. The terms contributing in these earlier expansions have been illustrated diagrammatically. There are connected and disconnected diagrams and their evaluation involves restricted lattice sums where two vertices must not coincide. Clearly, an expansion involving restricted lattice sums is not suitable for renormalization, because diagrammatic insertions interfere.

Hubbard[13] outlined an unrenormalized diagrammatic perturbation expansion of Green's functions in powers of intersite amplitudes for a general multiband lattice model. In his approach, a direct generalization of the so-called "linked-cluster expansion" for spin models,[4] only *connected diagrams* with *unrestricted lattice sums* are involved. Unfortunately, Hubbard's theory is obscured by the many details of the model he discusses, and the ensuing diagrammatic rules are very complicated. In fact, Hubbard discussed no explicit application of his expansion except for a reformulation of his earlier Green's-function decoupling approximation.[6] Furthermore, he did not derive a direct expansion of the grand-canonical potential Ω. Although Ω can in principle be calculated from the one-particle Green's function, a direct expansion of Ω is often simpler.

It is therefore worthwhile to rederive Hubbard's ex-

pansion for the special but important case of the single-band Hubbard model, including a direct expansion of the grand-canonical potential. This will be done in Sec. II of the present work, where we derive diagrammatic rules for the calculation of Ω and of one- and two-particle Green's functions in powers of t_{ij}, valid for arbitrary interaction strengths, particle densities, and lattice structures. These rules reduce the calculation of finite-order contributions to simple algebra, which can be performed by a computer program. This opens the way to the method of series extrapolation from high-finite-order calculations. We will also discuss the drastic simplifications arising in the strong-coupling limit $U\rightarrow\infty$. The discrepancies in the above-mentioned earlier expansions will be clarified.

In. Sec. III we derive the vertex-renormalized version of the perturbation expansion. This renormalization is obtained by generalizing the vertex renormalization for the linked-cluster expansion of the Ising model. The renormalized theory provides a basis for the construction of self-consistent approximations beyond finite-order perturbation theory. The criterion of self-consistency has been ignored in many approximate solutions of fermionic lattice models, but its importance is now being realized.[14]

In Sec. IV the perturbation expansion will be applied to the infinite-dimensional Hubbard model,[15] which has met with great interest recently.[16] In this limit only those embeddings of a diagram on the lattice contribute which have a fully two-particle reducible topology. As a consequence, the single-particle properties of the infinite-dimensional Hubbard model can be described in terms of independent tight-binding electrons hopping between renormalized ("dressed") Hubbard atoms. For the half-filled-band case, a ground-state perturbation expansion in powers of t_{ij}/U around the Néel state can be obtained by slightly modifying the finite-temperature theory. A conclusion in Sec. V closes the presentation.

II. PERTURBATION EXPANSION

In this section we derive the unrenormalized perturbation expansion for the Hubbard model,[5–7]

$$H=H_0+H_1 , \tag{1a}$$

where

$$H_0=U\sum_i n_{i\uparrow}n_{i\downarrow} \tag{1b}$$

is a local interaction of strength U and a kinetic-energy part,

$$H_1=\sum_{ij,\sigma} t_{ij}c^{\dagger}_{i\sigma}c_{j\sigma} , \tag{1c}$$

describes intersite hopping transitions, i.e., t_{ij} is the matrix element for a hopping process from a site $\mathbf{j}$ to a site $\mathbf{i}$. The operator $c^{\dagger}_{i\sigma}$ ($c_{i\sigma}$) creates (annihilates) a fermion with spin σ on a site $\mathbf{i}$ and $n_{i\sigma}=c^{\dagger}_{i\sigma}c_{i\sigma}$ is the local number operator for spin-σ fermions. Instead of H_0 (1b), one may also consider the generalization

$$H_0=\sum_i U_i n_{i\uparrow}n_{i\downarrow}+\sum_{i,\sigma} h_{i\sigma}n_{i\sigma} , \tag{1d}$$

where U_i is a site-dependent interaction and $h_{i\sigma}$ a site- and spin-dependent external field; the subsequent analysis is equally valid in this more general case.

The perturbation expansion will be set up at finite temperatures and a grand-canonical ensemble will be used. We define a grand-canonical Hamiltonian K by

$$K=K_0+K_1 , \tag{2a}$$

$$K_0=H_0-\mu\sum_{i,\sigma} n_{i\sigma} , \tag{2b}$$

$$K_1=H_1 , \tag{2c}$$

where μ is the chemical potential.

For $t_{ij}=0$ ("atomic limit") the model is easily solved because in this case $K=K_0$ is just a sum of local operators, each acting on a four-state "atom." In the following the (nonlocal) kinetic energy K_1 will be treated perturbatively by expanding the grand-canonical potential and dynamical correlation functions (Green's functions) in powers of the hopping matrix t_{ij}.

A. Grand-canonical potential

The grand-canonical potential is given by

$$\Omega=-T\ln \mathrm{tr}\, e^{-\beta K} , \tag{3}$$

where T is the temperature and $\beta=1/T$. The perturbation expansion is obtained from the interaction representation[17]

$$\Omega=\Omega_0-T\ln\langle\hat{S}\rangle_0 , \tag{4}$$

where Ω_0 is the grand-canonical potential corresponding to K_0 and

$$\langle\cdots\rangle_0=\mathrm{tr}\{\rho_0\cdots\} ,$$

$$\rho_0=\exp(-\beta K_0)/\mathrm{tr}\exp(-\beta K_0)$$

is the unperturbed ensemble average; the operator $\hat{S}$ is given by

$$\hat{S}=\mathcal{T}\exp\left[-\int_0^{\beta}d\tau\sum_{ij,\sigma} t_{ij}\hat{c}^{\dagger}_{i\sigma}(\tau)\hat{c}_{j\sigma}(\tau)\right] , \tag{5}$$

where $\mathcal{T}$ denotes the (imaginary-) time-ordering operator and

$$\hat{c}^{\dagger}_{i\sigma}(\tau)=e^{K_0\tau}c^{\dagger}_{i\sigma}e^{-K_0\tau} , \tag{6a}$$

$$\hat{c}_{i\sigma}(\tau)=e^{K_0\tau}c_{i\sigma}e^{-K_0\tau} \tag{6b}$$

are the creation and annihilation operators in (imaginary-time) interaction representation. Expanding the exponential in (5), one obtains for the nth-order contribution to $\langle\hat{S}\rangle_0$:

$$\frac{(-1)^n}{n!}\sum_{j_1\cdots j_n,j_1'\cdots j_n'} t_{j_1'j_1}\cdots t_{j_n'j_n}\sum_{\sigma_1\cdots\sigma_n}\int_0^\beta d\tau_1\cdots d\tau_n\langle \mathcal{T}[\hat{c}^\dagger_{j_1'\sigma_1}(\tau_1)\hat{c}_{j_1\sigma_1}(\tau_1)\ldots\hat{c}^\dagger_{j_n'\sigma_n}(\tau_n)\hat{c}_{j_n\sigma_n}(\tau_n)]\rangle_0 . \tag{7}$$

The ensemble average $\langle\ldots\rangle_0$ appearing in (7) is just the n-particle Green's function of the *unperturbed* system

$$G_n^0(\mathbf{j}_1\tau_1\sigma_1,\ldots,\mathbf{j}_n\tau_n\sigma_n|\mathbf{j}_1'\tau_1'\sigma_1',\ldots,\mathbf{j}_n'\tau_n'\sigma_n')=\langle \mathcal{T}[\hat{c}^\dagger_{\mathbf{j}_1'\sigma_1'}(\tau_1')\hat{c}_{\mathbf{j}_1\sigma_1}(\tau_1)\ldots\hat{c}^\dagger_{\mathbf{j}_n'\sigma_n'}(\tau_n')\hat{c}_{\mathbf{j}_n\sigma_n}(\tau_n)]\rangle_0 \tag{8}$$

evaluated at $\tau_i=\tau_i'$, $\sigma_i=\sigma_i'$. To condense the notation, we abbreviate $\mathbf{j}_1,\tau_1,\sigma_1$ by 1, $\mathbf{j}_1',\sigma_1',\tau_1'$ by 1′, etc.

The Green's function $G_n^0(1,\ldots,n|1',\ldots,n')$ can be written as a sum of products of cumulants (connected Green's functions) C_m^0, where each term of the sum corresponds to a partition of $(1,\ldots,n,1',\ldots,n')$ in subsets containing equal numbers of primed and unprimed variables,[18] e.g.,

$$G_1^0(1|1')=C_1^0(1|1') , \tag{9a}$$

$$G_2^0(1,2|1',2')=C_2^0(1,2|1',2')+C_1^0(1|1')C_1^0(2|2')-C_1^0(1|2')C_1^0(2|1') . \tag{9b}$$

The sign attached to a product is determined by the parity of the permutation of the primed variables with respect to the unprimed variables.

The cumulants can also be obtained by calculating functional derivatives of the generating functional

$$C_0^0\{\xi^*,\xi\}=\ln\left\langle \mathcal{T}\exp\left[-\sum_{j,\sigma}\int_0^\beta d\tau[\xi^*_{j\sigma}(\tau)\hat{c}_{j\sigma}(\tau)+\hat{c}^\dagger_{j\sigma}(\tau)\xi_{j\sigma}(\tau)]\right]\right\rangle_0 \tag{10}$$

with respect to the Grassmann fields ξ,ξ^*:[18]

$$C_m^0(1,\ldots,m|1',\ldots,m')=\frac{\delta}{\delta\xi^*(1)}\cdots\frac{\delta}{\delta\xi^*(m)}\frac{\delta}{\delta\xi(m')}\cdots\frac{\delta}{\delta\xi(1')}C_0^0\{\xi^*,\xi\}\Big|_{\xi=\xi^*=0} . \tag{11}$$

The ensemble average $\langle\cdots\rangle_0$ in (10) factorizes into independent local averages (one for each site $\mathbf{j}$) because K_0 is a sum of local operators. Hence, $C_0^0\{\xi^*,\xi\}$ is a sum of local functionals

$$C_0^0\{\xi^*,\xi\}=\sum_j C_{0j}^0\{\xi_j^*,\xi_j\} , \tag{12}$$

where $C_{0j}^0\{\xi_j,\xi_j\}$ is obtained from (10) by omitting the lattice sum. As a consequence of (12), the unperturbed cumulants C_m^0 are local (site diagonal), i.e., they vanish if not all site variables in $(1,\ldots,m|1',\ldots,m')$ are equal. The mth-order cumulants at $\mathbf{j}$ will henceforth be denoted by

$$C_{mj}^0(s_1,\ldots,s_m|s_1',\ldots,s_m') ,$$

where $s_i=(\tau_i,\sigma_i)$ and $s_i'=(\tau_i',\sigma_i')$ collect time and spin variables.

The explicit calculation of Ω becomes much clearer when the terms of the expansion are represented diagrammatically.[13] A cumulant

$$C_{mj}^0(s_1,\ldots,s_m|s_1',\ldots,s_m')$$

is represented by a $2m$-valent point vertex (labeled by $\mathbf{j}$) which is attached to m entering lines (labeled by $s_1',\ldots,s_m'$) and m leaving lines (labeled by $s_1,\ldots,s_m$); a directed line running from a vertex $\mathbf{j}$ to a vertex $\mathbf{i}$ corresponds to a hopping matrix element t_{ij}. In Fig. 1 the diagrams yielding the leading-order contributions to Ω are shown (disconnected diagrams do not contribute to Ω; see below).

In nth order there are $n!/g(D)$ different partitions (contributing to the cumulant decomposition of G_n^0) leading to the same diagram D. The *symmetry factor* $g(D)$ is defined as the number of distinct permutations of labeled lines and vertices which do not alter the topological structure of the diagram D. For example, an nth-order polygon (diagrams 2a–4a in Fig. 1) is generated by partitions of the form $C_1^0(1|P1')C_1^0(2|P2')\ldots C_1^0(n|Pn')$, where P is a permutation. Clearly, there are $(n-1)!$ distinct proper partitions. On the other hand, the symmetry factor g of an nth-order (directed) polygon is n, i.e., $n!/g=(n-1)!$, as expected. Cancelling the factor $1/n!$ emerging from the expansion of the exponential [see (7)], each diagram D acquires simply a prefactor $1/g(D)$.

The *sign* associated with a diagram is determined by the following procedure.[13] Imagine each entering line at a vertex to be paired with an arbitrary line leaving this vertex (see Fig. 2). In this way the diagram is divided into a set of loops. The time-spin arguments of a cumulant

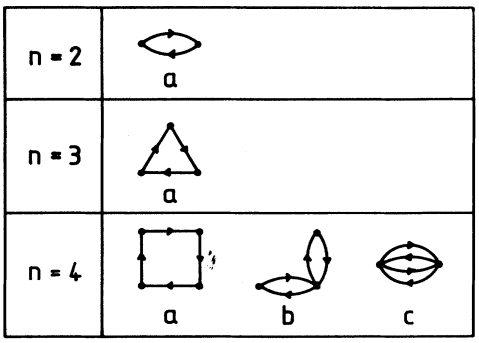

FIG. 1. Diagrams contributing to Ω for the leading orders $n=2,3,4$.

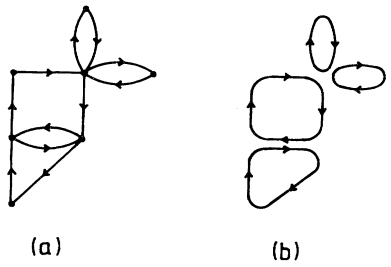

FIG. 2. Fixing the number of loops by line pairing in a diagram: (a) diagram, (b) separated loops.

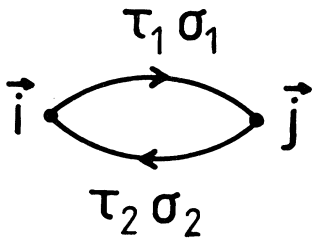

FIG. 3. Diagram contributing to Ω_2.

$$C^0_{mj}(s_1,\ldots,s_m|s'_1,\ldots,s'_m)$$

associated with a vertex must be arranged such that s_i and s'_i label paired lines (for all i). Then the overall sign of a diagram is simply $(-1)^f$, where f is the number of loops. This rule is easily verified for partitions of

$$G^0_n(1,\ldots,n|1',..,n')$$

without permutations, i.e., for partitions of the form

$$C^0_{m_1}(1,\ldots,m_1|1',\ldots,m'_1)C^0_{m_2}[m_1+1,\ldots,m_1+m_2|(m_1+1)',\ldots,(m_1+m_2)']\ldots;$$

the general validity follows from the simple observation that each transmutation of arguments, e.g., $1\leftrightarrow m_1+1$, changes the number of loops of the corresponding diagram by one. Note that the factor $(-1)^n$ from (7) has already been included in our sign rule.

Clearly, the contribution of a disconnected diagram is just the product of the contributions of its connected components. This is because the lattice sums in (7) are unrestricted, i.e., different vertices are allowed to be on the same lattice site. Hence the *linked-cluster theorem*[19] applies, i.e., $\ln\langle\hat{S}\rangle_0$ is given by the sum of all *connected diagrams*.

We are now in a position to state the diagrammatic rule for the calculation of Ω.

Rule 1: Grand-canonical potential Ω.

(a) Draw all topologically distinct connected diagrams D composed of directed lines and point vertices in such a way that at each vertex the number of entering lines equals the number of leaving lines.

(b) Label each line with an (imaginary) time and a spin variable; label each vertex with a lattice vector.

(c) Each line running from a vertex **i** to a vertex **j** yields a factor t_{ij}; each vertex **j** with m entering lines (labeled by $s'_1,\ldots,s'_m$) and m leaving lines (labeled by $s_1,\ldots,s_m$) yields a factor

$$C^0_{mj}(s_1,\ldots,s_m|s'_1,\ldots,s'_m)\ .$$

(d) Determine the sign of each diagram (plus/minus for an even/odd number of loops).

(e) Determine the symmetry factor $g(D)$ for each diagram, i.e., the number of distinct permutations of (labeled) vertices and lines which do not alter the topological structure of the diagram.

(f) For each diagram D, multiply the hopping matrix elements and cumulants obtained in (c), integrate each time variable from 0 to β, and sum each spin variable and sum each lattice vector over the whole lattice; multiplying the result by the sign and dividing by the symmetry factor of D, one obtains a quantity $w(D)$, which we refer to as the "weight" of D.

The grand-canonical potential Ω is then given by

$$\Omega=\Omega_0-T\sum_D w(D)\ , \tag{13}$$

where the sum extends over all connected diagrams.

Clearly, the nth-order contribution Ω_n is obtained from those diagrams which contain exactly n lines. We note that, since $t_{ii}=0$, there are no diagrams where a single line forms a loop.

As an example, we calculate the second-order contribution Ω_2. There is only one diagram contributing in this order (quadratic in the hopping matrix), which we label as shown in Fig. 3. The diagram has one loop (the pairing of lines at the vertices is unique in this case) and its symmetry factor is 2. Hence,

$$w(D)=-\tfrac{1}{2}\sum_{i,j}\sum_{\sigma_1,\sigma_2}\int_0^\beta d\tau_1 d\tau_2 t_{ij}t_{ji}C^0_{1i}(\tau_1\sigma_1|\tau_2\sigma_2)C^0_{1j}(\tau_2\sigma_2|\tau_1\sigma_1)\ , \tag{14}$$

where C^0_1 is the atomic one-particle Green's function which, for H_0, (1d), is given by

$$C^0_{1i}(\tau\sigma|\tau'\sigma')=\delta_{\sigma\sigma'}\Theta(\tau'-\tau)(p^0_{\sigma i}+p^0_{di}e^{-U_i(\tau-\tau')})e^{-(h_{i\sigma}-\mu)(\tau-\tau')}-\delta_{\sigma\sigma'}\Theta(\tau-\tau')(p^0_{ei}+p^0_{-\sigma i})e^{-(h_{i\sigma}-\mu)(\tau-\tau')}\ . \tag{15}$$

Here, $p^0_{ei}, p^0_{\sigma i}, p^0_{-\sigma i}, p^0_{di}$ are the local densities of empty, singly occupied (spin σ or $-\sigma$), and doubly occupied sites, respectively (calculated in the atomic limit). Inserting (15) in (13) and (14), one obtains, for site-independent $U_i = U$ and $h_{i\sigma} = h_\sigma$,

$$\Omega_2 = -\tfrac{1}{2}\sum_{i,j} t_{ij}^2 [\beta(p^0_\sigma + p^0_{-\sigma})(p^0_e + p^0_d) + \frac{4}{U}(p^0_\sigma p^0_{-\sigma} - p^0_e p^0_d)] \ . \tag{16}$$

The evaluation of diagrams is often simplified by using the frequency representation of the cumulants

$$C^0_{mj}(\tau_1\sigma_1, \ldots, \tau_m\sigma_m | \tau'_1\sigma'_1, \ldots, \tau'_m\sigma'_m)$$
$$= \beta^{-m} \sum_{\omega_1, \ldots, \omega_m, \omega'_1, \ldots, \omega'_m} e^{-i(\omega_1\tau_1 + \cdots - \omega'_1\tau'_1 - \cdots)} C^0_{mj}(\omega_1\sigma_1, \ldots, \omega_m\sigma_m | \omega'_1\sigma'_1, \ldots, \omega'_m\sigma'_m) \ , \tag{17}$$

where ω_i, ω'_i are fermionic Matsubara frequencies [$\omega_i = \pi T(2n_i + 1)$, $\omega'_i = \pi T(2n'_i + 1)$, where n_i, n'_i are integers]. The inverse transformation is

$$C^0_{mj}(\omega_1\sigma_1 \ldots \omega_m\sigma_m | \omega'_1\sigma'_1, \ldots, \omega'_m\sigma'_m)$$
$$= \beta^{-m} \int_0^\beta d\tau_1 \ldots d\tau_m d\tau'_1 \ldots d\tau'_m e^{i(\omega_1\tau_1 + \cdots - \omega'_1\tau'_1 - \cdots)} C^0_{mj}(\tau_1\sigma_1, \ldots, \tau_m\sigma_m | \tau'_1\sigma'_1, \ldots, \tau'_m\sigma'_m) \ . \tag{18}$$

Inserting (17) for the vertices of a diagram, one can easily carry out the time integrals [see Rule 1(f)]. This yields a Fourier-transformed version of Rule 1 where lines are labeled by Matsubara frequencies (instead of time variables), cumulants are inserted in frequency representation, and finally Matsubara sums (instead of time integrals) are carried out. There is frequency conservation at the vertices since

$$C^0_{mj}(\omega_1\sigma_1, \ldots, \omega_m\sigma_m | \omega'_1\sigma'_1, \ldots, \omega'_m\sigma'_m) = 0 \ ,$$

if

$$\omega_1 + \cdots + \omega_m - \omega'_1 \cdots - \omega'_m \neq 0 \ . \tag{19}$$

In the absence of site-dependent external fields and for constant $U_j = U$, the atomic cumulants $C^0_{mj}(\ldots)$ do not depend on j, i.e., we may drop the site index, writing $C^0_m(\ldots)$. In this case the vertices of a diagram are site independent while the lines are (always) time independent, i.e., space and time dependences factorize. One may define a *temporal weight* $w_t(D)$ of a diagram by inserting a factor 1 for each line, summing only spin and time variables (no site variables), and attaching the sign given by the number of loops. The *spatial weight* $w_s(D)$ is obtained by inserting factors 1 for the vertices, summing the site indices (not spin and time), and dividing by the symmetry factor. Clearly, the *total weight* $w(D)$ is then given by the product $w_s(D)w_t(D)$. Note that $w_s(D)$ is independent of K_0 (in particular, it is independent of U and μ) while $w_t(D)$ is independent of the lattice structure.

The calculation of the lattice sums for a diagram becomes particularly simple in the case of pure next-neighbor hopping, i.e., for $t_{ij} = -t$ if i, j are next neighbors on the lattice and $t_{ij} = 0$, otherwise. In this case the lattice sum amounts to calculating the *free multiplicity* $m(D)$ of the diagram, i.e., the number of distinct ways (per site) in which the vertex-labeled diagram can be embedded in the lattice with each vertex assigned to a site of the lattice and each line lying along a next-neighbor bond. Different vertices may coincide on the same lattice site. There are efficient "computerizable" algorithms for the calculation of lattice constants, such as the free multiplicity.[20]

As an example, we outline the calculation of the fourth-order grand-canonical potential Ω_4 for next-neighbor hopping on a d-dimensional hypercubic lattice. In this case the diagrams D_{4a}, D_{4b}, and D_{4c} in Fig. 1 contribute. The symmetry factors are 4, 2, and 8, respectively, and the free multiplicities are $2d(6d-3)$, $(2d)^2$, and $2d$, respectively. Using Rule 1, one obtains the following contributions to Ω:

$$\Omega_{4a} = -LT\frac{d}{2}(6d-3)t^4 \sum_{r_1} [C^0_1(r_1|r_1)]^4 \ ,$$

$$\Omega_{4b} = LT(2d^2)t^4 \sum_{r_1, r_2} C^0_1(r_1|r_1) C^0_2(r_1, r_2|r_1, r_2) \times C^0_1(r_2|r_2) \ ,$$

$$\Omega_{4c} = LT\frac{d}{4}t^4 \sum_{r_1, r_2, r_3} C^0_2(r_1, r_3|r_2, r_1 + r_3 - r_2) \times C^0_2(r_2, r_1 + r_3 - r_2|r_1, r_3) \ , \tag{20}$$

where the variables r_i include both spin and frequency variables; spin and frequency conservation at the vertices has already been built in; L is the number of lattice sites. The lines at the two-particle vertices in D_{4b}, D_{4c} have been paired such that two loops result. The atomic one-particle cumulant in frequency representation reads

$$C^0_{1i}(\omega\sigma|\omega\sigma) = \frac{p^0_{ei} + p^0_{\sigma i}}{i\omega + \mu - h_{i\sigma}} + \frac{p^0_{ei} + p^0_{di}}{i\omega + \mu - h_{i\sigma} - U_i} \ . \tag{21}$$

The expression for the atomic two-particle cumulant is too lengthy to be presented here. Its calculation and the evaluation of the Matsubara sum in (20) is, however, straightforward. The correct result for Ω_4 has already been derived by Kubo,[8] who used a different technique. We note that the fourth-order grand-canonical potential

of the Hubbard model has already been investigated by several other authors, all arriving at different results.[9,10,12] In Ref. 10 the error is due to an unwarranted application of the linked-cluster theorem. In Refs. 9 and 12 the minus signs ensuing from permutations of fermions have not been taken into account.

For $U=\infty$ the spin and charge degrees of freedom in the partition function of the one-dimensional Hubbard model with next-neighbor hopping are known to separate.[21] Hence, the partition function (in the presence of a homogeneous magnetic field h) can be written as

$$Z=\prod_k (1+e^{\beta(\varepsilon_k+h-\mu)}+e^{\beta(\varepsilon_k-h-\mu)}) , \tag{22}$$

where $\varepsilon_k=-2t\cos k$ is the one-dimensional tight-binding band structure and the k product extends over the Brillouin zone. This yields

$$\Omega=\Omega_0-LT\int_{-1}^{1}\frac{dx}{\pi(1-x^2)^{1/2}}\ln[p_e^0+(p_\sigma^0+p_{-\sigma}^0)e^{-2t\beta x}] . \tag{23}$$

We checked our (and Kubo's) result for Ω_4 by expanding Ω (23) in powers of t and comparing coefficients.

B. Green's functions

The one-particle thermal Green's function is given by

$$G_{\sigma jj'}(\tau,\tau')=-\mathrm{tr}\{\rho\mathcal{T}[\tilde{c}_{j\sigma}(\tau)\tilde{c}^{\dagger}_{j'\sigma}(\tau')]\} , \tag{24}$$

where

$$\rho=\exp(-\beta K)/\mathrm{tr}\exp(-\beta K)$$

is the statistical operator for K and

$$\tilde{c}^{\dagger}_{j\sigma}(\tau)\equiv e^{K\tau}c^{\dagger}_{j\sigma}e^{-K\tau} , \tag{25a}$$

$$\tilde{c}_{j\sigma}(\tau)\equiv e^{K\tau}c_{j\sigma}e^{-K\tau} \tag{25b}$$

are the creation and annihilation operators in Heisenberg representation with respect to K.

The perturbation expansion of $G_{\sigma jj'}(\tau,\tau')$ is closely analogous to that of Ω and we will therefore sketch its derivation rather briefly. The perturbation expansion is generated from the interaction representation

$$G_{\sigma jj'}(\tau,\tau')=-\langle\mathcal{T}[\hat{c}_{j\sigma}(\tau)\hat{c}^{\dagger}_{j'\sigma}(\tau')\hat{\mathcal{S}}]\rangle_0/\langle\hat{\mathcal{S}}\rangle_0 , \tag{26}$$

where $\hat{\mathcal{S}}$ is given by (5). The numerator of (26) can be expanded in powers of the hopping matrix where the coefficients are expressible in terms of atomic cumulants C_m^0. Each term can be represented by a diagram by associating vertices with the cumulants and lines with the hopping matrices. The diagrams differ from those for Ω in that they are *rooted*, i.e., there are one or two *external vertices*, which have fixed site indices and some fixed time and spin indices (the other vertices will be referred to as *internal vertices*). The appearance of external vertices is due to the operators $\hat{c}_{j\sigma}(\tau),\hat{c}^{\dagger}_{j'\sigma}(\tau')$ in (26), which have fixed site, time, and spin variables.

The rules for the sign and the symmetry factor of a diagram are the same as those for Ω. The contribution of a disconnected diagram is again just the product of the contributions of its connected components. Hence, the linked-cluster theorem applies,[13] which in this case states that the disconnected diagrams appearing in the numerator of (26) are cancelled by the denominator $\langle\hat{\mathcal{S}}\rangle_0$ of (26). Thus, we end up with the following rules for the calculation of the one-particle Green's function:

Rule 2: One-particle Green's function $G_{\sigma jj'}(\tau,\tau')$.

(a) Draw all topologically distinct connected diagrams D composed of point vertices, directed "internal" lines (connecting two vertices), and two "external lines" (one entering and one leaving a vertex) such that at each vertex the number of entering lines equals the number of leaving lines (see Fig. 4).

(b) Label each line with a time and a spin variable, the entering external line is labeled by τ',σ; the leaving one by τ,σ. Label each vertex with a lattice vector, the vertex with the entering external line is labelled by j', the one with the leaving line by j (the external vertices may coincide: in this case j=j').

(c)–(e) Same as in Rule 1.

(f) Same as for Rule 1, except that now only the time and spin variables on internal lines and the site labels of internal vertices are summed, while the labels of external lines and vertices are kept fixed. The one-particle Green's function is finally given by the sum of the weights $w(D)$ of all diagrams D:

$$G=\sum_D w(D) . \tag{27}$$

The Fourier transform $G_{\sigma jj'}(\omega)$ of $G_{\sigma jj'}(\tau,\tau')$ is obtained by using the Fourier-transformed version of Rule 2,

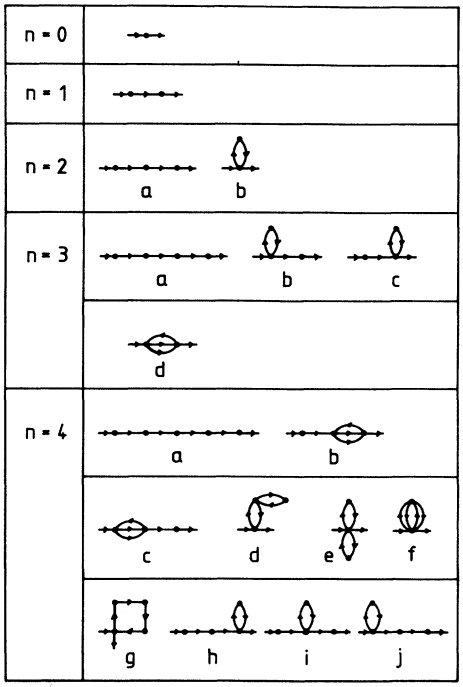

FIG. 4. Diagrams contributing to the one-particle Green's function G for next-neighbor hopping on a hypercubic lattice (up to fourth order).

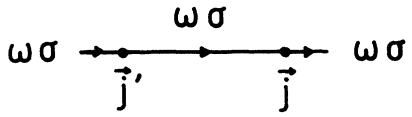

FIG. 5. Diagram contributing to G^1.

where internal lines carry dummy (Matsubara) frequency variables which are summed while both external lines carry the fixed frequency ω. For translational invariance and next-neighbor hopping, the evaluation of the lattice sum for a diagram D again (as for Ω) reduces to the calculation of the free multiplicity $m(D)$.

To illustrate Rule 2, we calculate the first-order (in t_{ij}) contribution G^1 to the one-particle Green's function. The only first-order diagram is shown in Fig. 5. There are no loops and the symmetry factor is 1. Following (the Fourier-transformed version of) Rule 2, one obtains

$$G^1_{\sigma jj'}(\omega)=t_{jj'}C^0_{1j}(\omega\sigma|\omega\sigma)C^0_{1j'}(\omega\sigma|\omega\sigma)\ , \tag{28}$$

where C^0_1 is the atomic one-particle cumulant as given by (21).

As a second example, we evaluate the second-order diagram D_{2b} shown in Fig. 6. Pairing the internal lines at

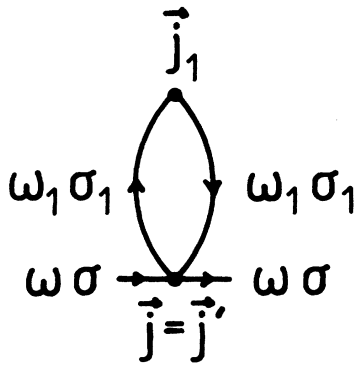

FIG. 6. Diagram contributing to G^2.

the two-particle vertex, one obtains one loop; the symmetry factor is 1. Hence, Rule 2 yields

$$G^{2b}_{\sigma jj'}(\omega)=-\delta_{jj'}\sum_{j_1}t_{jj_1}t_{j_1j}\sum_{r_1}C^0_{2j}(r,r_1|r,r_1)C^0_{1j_1}(r_1|r_1)\ . \tag{29}$$

The generalization of Rule 2 to many-particle Green's functions is straightforward. The n-particle Green's function

$$G_n(1,\ldots,n|1',\ldots,n')=\langle\mathcal{T}[\tilde{c}^{\dagger}_{j'_1\sigma'_1}(\tau'_1)\tilde{c}_{j_1\sigma_1}(\tau_1)\ldots\tilde{c}^{\dagger}_{j'_n\sigma'_n}(\tau'_n)\tilde{c}_{j_n\sigma_n}(\tau_n)]\rangle \tag{30}$$

can be written in terms of cumulants (connected Green's functions) $C_m(1,\ldots,m|1',\ldots,m')$. In particular,

$$G_2(1,2|1',2')=C_2(1,2|1',2')+C_1(1|1')C_1(2|2')-C_1(1|2')C_1(2|1')\ , \tag{31}$$

where $C_1=G_1=G$ is the one-particle Green's function. From G_2 (or C_2) all two-particle correlation functions can be calculated. The m-particle cumulant is obtained by applying

Rule 3: m-particle cumulant

$$C_m(1,\ldots,m|1',\ldots,m')\ .$$

Same as Rule 2 except that now there are m entering and m leaving external lines carrying fixed time and spin variables and fixing the site variables of those vertices which are connected to external lines. Apart from the internal time, spin, and lattice sums, the evaluation of a diagram contributing to $C_m(1,\ldots,m|1',\ldots,m')$ involves a sum over all permutations of the external variables $(1,\ldots,m)$ and $(1',\ldots,m')$, respectively. The sign of a diagram is again determined by line pairing (see above), which now separates the diagram in loops and in chains connecting the lth entering external line with the Plth external leaving line (for $l=1,\ldots,m$) where P is a permutation. The sign is $(-1)^f\epsilon_P$, where f is the number of loops and ϵ_P is the sign of P.

The diagrams contributing in leading order to the two-particle cumulant C_2 are shown in Fig. 7.

C. Special case $U=\infty$

In many systems the local interaction U is much larger than any other energy scale. Therefore, several works have focused on the strong interaction limit $U\to\infty$ of the Hubbard model.

In the limit $U\to\infty$ all states with doubly occupied sites are suppressed. In the remaining subspace of the Hilbert space there are only three possible states on each site: empty, spin up, or spin down. The interaction H_0, (1b), of the Hubbard model is zero in this subspace.

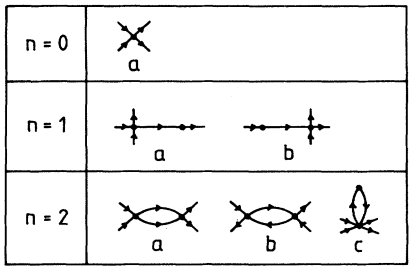

FIG. 7. Diagrams contributing to the two-particle cumulant C_2 for the leading orders $n=0,1,2$.

Hence, the atomic cumulants become much simpler for $U=\infty$:

$$C^0_{mj}(s_1,\ldots,s_m|s'_1,\ldots,s'_m) = e^{\mu(\tau_1-\tau'_1+\cdots+\tau_m-\tau'_m)}\chi_m(s_1,\ldots,s_m|s'_1,\ldots,s'_m)\ , \tag{32}$$

where χ_m depends only on the spins and on the *time order* of the time variables.

In a diagram, a factor $\exp(\mu\tau_i)$ resulting from a vertex where a line (with a time label τ_i) is leaving is cancelled by a factor $\exp(-\mu\tau_i)$ which is due to the vertex where this line ends. Only the exponentials corresponding to external lines remain. Thus, for a given time order, the product of cumulants in a diagram is independent of the internal time variables. Hence, the time integration within the region defined by a certain time order yields just the volume of that region.

As an example, we consider the calculation of the grand-canonical potential Ω as described by Rule 1. Each time integration in an nth-order diagram over the region defined by a certain time order yields a factor

$$\int_0^\beta d\tau_1\ldots d\tau_n\Theta(\tau_{P1},\tau_{P2}\ldots\tau_{Pn})=\beta^n/n!\ , \tag{33}$$

where P is an arbitrary permutation of $(1,\ldots,n)$ and

$$\Theta(\tau_{P1},\tau_{P2},\ldots,\tau_{Pn})=1$$

for $\tau_{P1}>\tau_{P2}>\ldots>\tau_{Pn}$ and 0 otherwise. Hence, the time integration in a diagram reduces to a sum over all possible time orders, i.e., over all permutations of $(1,\ldots,n)$:

$$\int_0^\beta d\tau_1,\ldots,d\tau_n\ldots=\frac{\beta^n}{n!}\sum_P\ldots\ . \tag{34}$$

The evaluation of a diagram has therefore been reduced to the calculation of *finite* sums, which can be performed by a simple computer program.

To further cross check our method and the results for Ω obtained by Kubo and Tada,[11] we have calculated Ω for $U=\infty$ up to sixth order in the hopping matrix t (for next-neighbor hopping) on a d-dimensional hypercubic lattice. The results agree with those of Kubo and Tada (published for $d=1,2,3$). For $d=1$ they also agree with the corresponding nth-order contributions obtained by expanding the exact Ω (23) in powers of t.

D. Discussion

The perturbation theory developed so far enables one to calculate the leading corrections to the atomic limit of the Hubbard model in a particularly transparent manner. A glance at the number of incorrect results obtained earlier[9,10,12] suffices to convince oneself of the usefulness of uniquely defined diagrammatic rules describing the calculation of an nth-order contribution. The rules also provide an illustrative real-space picture of the dynamics of fermions in the Hubbard model in terms of time-ordered lattice walks. Clearly, a perturbation expansion terminated at some finite order is applicable only when the hopping matrix t_{ij} is small compared to the temperature T, i.e., either for very narrow bands or for extremely high temperatures.

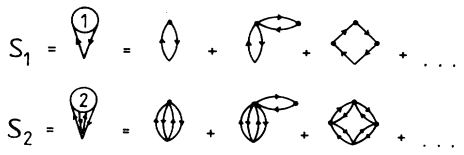

FIG. 8. The self-fields S_1 and S_2.

One way to go beyond perturbation theory is to extrapolate finite-order contributions to infinite order by applying appropriate extrapolation techniques such as Padé approximants or ratio methods.[22] Series extrapolation methods have been successfully applied to models with localized spins,[3] while for correlated lattice fermions this approach has so far not been exhausted.[23] Clearly, a sufficiently large number of orders must be evaluated to allow for a reliable extrapolation. For this a "computerizable" algorithm is indispensable and this is exactly what the above diagrammatic rules provide.

Nonperturbative approximations can be obtained by summing an infinite subclass of diagrams. The selection of diagrams may be guided by physical intuition or, more safely, by a small parameter (different from the expansion parameter). A naive choice of diagrams usually leads to approximations which violate conservation laws, sum rules, etc. The vertex renormalization described in Sec. III will provide a basis for the construction of self-consistent approximations.

III. VERTEX RENORMALIZATION

The purpose of the vertex renormalization is to absorb all possible local insertions at a bare vertex into a renormalized vertex, thus yielding an expansion of Green's functions in terms of diagrams in which all local insertions are removed. The vertex renormalization described here is closely analogous to that known for the linked-cluster expansion of the Ising model.[4]

To classify the various types of insertions at a vertex, we define an n-particle *self-field*

$$S_{nj}(s_1,\ldots,s_n|s'_1,\ldots,s'_n)\ ,$$

as a sum over all connected n-particle insertions at j as indicated for S_1 and S_2 in Fig. 8. The external vertex of a self-field diagram (the one without a dot in Fig. 8) bears no cumulant and the lines incident at this vertex have fixed time and spin variables (namely, $s_1,\ldots,s_n,s'_1,\ldots,s'_n$). An insertion is "connected" if it

FIG. 9. Definition of the renormalized atomic two-particle cumulant $\bar{C}_2$.

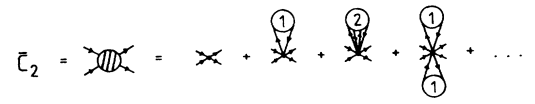

FIG. 10. $\bar{C}_2$ in terms of the self-fields.

cannot be decomposed in disconnected parts by just separating the lines fixed to the external vertex. Apart from the special treatment of the external vertex, the evaluation of a self-field diagram proceeds exactly as for the Green's-function diagrams (see Rules 2 and 3).

To remove local insertions from the diagrammatic perturbation expansion, we define a *renormalized m-particle cumulant*

$$\bar{C}_{m\mathrm{j}}(s_1,\ldots,s_m|s'_1,\ldots,s'_m)$$

as the sum of all possible insertions that can be attached to an m-particle vertex. This is illustrated in Fig. 9 (for $m=2$). Clearly, $\bar{C}_m$ can be expressed in terms of self-fields and bare vertices, as described diagrammatically in Fig. 10 (for $m=2$). Algebraically, we obtain

$$\bar{C}_{m\mathrm{j}}(\vec{s}|\vec{s}')=C^0_{m\mathrm{j}}(\vec{s}|\vec{s}')+\sum_{n_1}\int d\vec{s}_1 d\vec{s}'_1 C^0_{m+n_1,\mathrm{j}}(\vec{s},\vec{s}_1|\vec{s}',\vec{s}'_1)S_{n_1\mathrm{j}}(\vec{s}_1|\vec{s}'_1)$$
$$+\tfrac{1}{2}\sum_{n_1 n_2}\int d\vec{s}_1 d\vec{s}'_1 d\vec{s}_2 d\vec{s}'_2 C^0_{m+n_1+n_2,\mathrm{j}}(\vec{s},\vec{s}_1,\vec{s}_2|\vec{s}',\vec{s}'_1,\vec{s}'_2)S_{n_1\mathrm{j}}(\vec{s}_1|\vec{s}'_1)S_{n_2\mathrm{j}}(\vec{s}_2|\vec{s}'_2)+\cdots . \tag{35}$$

Here several time and/or spin variables have been collected in vectors, e.g., $\vec{s}=(s_1,\ldots,s_m)$; their dimension is defined by the context. The infinite sum (35) can be rewritten in a compact form by making use of the generating functional $C^0_{0\mathrm{j}}\{\xi,\xi^*\}$ defined by (10) and (12). Defining bare cumulants in the presence of Grassmann fields

$$C^0_{m\mathrm{j}}\{(\vec{s}|\vec{s}');\xi,\xi^*\}=\frac{\delta^m}{\delta\xi^*(\vec{s})}\frac{\delta^m}{\delta\xi(\vec{s}')}C^0_{0\mathrm{j}}\{\xi,\xi^*\} , \tag{36}$$

where

$$\frac{\delta^m}{\delta\xi^*(\vec{s})}=\frac{\delta}{\delta\xi^*(s_1)}\cdots\frac{\delta}{\delta\xi^*(s_m)} , \tag{37a}$$

$$\frac{\delta^m}{\delta\xi(\vec{s}')}=\frac{\delta}{\delta\xi(s'_m)}\cdots\frac{\delta}{\delta\xi(s'_1)} , \tag{37b}$$

one obtains

$$\bar{C}_{m\mathrm{j}}(\vec{s}|\vec{s}')$$
$$=\exp\left[\sum_{n=1}^{\infty}\int d\vec{s}_n d\vec{s}'_n S_{n\mathrm{j}}(\vec{s}_n|\vec{s}'_n)\frac{\delta^n}{\delta\xi^*(\vec{s}_n)}\frac{\delta^n}{\delta\xi(\vec{s}'_n)}\right]$$
$$\times C^0_{m\mathrm{j}}\{(\vec{s}|\vec{s}');\xi,\xi^*\}|_{\xi,\xi^*=0} . \tag{38}$$

In this way the renormalized cumulants $\bar{C}_m$ become functionals of the self-fields $S_1,S_2,\ldots$; from (38) one obtains the useful identity

$$\delta\bar{C}_{m\mathrm{j}}(\vec{s}|\vec{s}')/\delta S_{n\mathrm{j}}(\vec{s}_n|\vec{s}'_n)=\bar{C}_{m+n,\mathrm{j}}(\vec{s},\vec{s}_n|\vec{s}',\vec{s}'_n) . \tag{39}$$

The one-particle Green's function $G=C_1$ and the many-particle Green's functions can now be written as a sum over all diagrams without local insertions where renormalized cumulants $\bar{C}_m$ are inserted for the vertices. The leading terms contributing to G are shown in Fig. 11. It is easy to convince onself that the signs and symmetry factors involved in the evaluation of diagrams (see Rules 2 and 3) are treated correctly by the above resummation, i.e., there is no undercounting or overcounting of diagrams. It should be noted that for the renormalization procedure to work it is crucial to start from a diagrammatic expansion which involves *unrestricted lattice sums.*

To express the grand-canonical potential Ω in terms of renormalized cumulants, we define a functional $\Phi\{\bar{C}\}$ by

$$\Phi\{\bar{C}\}=\text{sum over all } \textit{closed diagrams} \text{ with } \textit{renormalized vertices } \bar{C}_m \text{ } \textit{without local insertions} . \tag{40}$$

The rules governing the evaluation of Φ are the same as those for Ω (Rule 1), except that now only diagrams without local insertions are involved and vertices correspond to renormalized cumulants instead of bare ones. Note that Φ is different from Ω since the former overcounts unrenormalized diagrams. However, Ω and Φ are related by the equation

$$\Omega=\Phi+\sum_{\mathrm{j}}\bar{C}_{0\mathrm{j}}$$
$$-\sum_{n=1}^{\infty}\sum_{\mathrm{j}}\int d\vec{s}_n d\vec{s}'_n S_{n\mathrm{j}}(\vec{s}_n|\vec{s}'_n)\bar{C}_{n\mathrm{j}}(\vec{s}_n|\vec{s}'_n) , \tag{41}$$

which is proved in the Appendix.

Clearly, the self-fields S_n can also be expanded in terms of diagrams with renormalized vertices $\bar{C}_m$. As for the Green's functions, there is no overcounting problem in this case. Hence, given the functional $\bar{C}_m\{S\}$, (38), local insertions are completely removed from the perturbation expansion. The self-fields can also be obtained by functionally differentiating $\Phi\{\bar{C}\}$:

$$S_{n\mathrm{j}}(\vec{s}_n|\vec{s}'_n)=\delta\Phi/\delta\bar{C}_{n\mathrm{j}}(\vec{s}_n|\vec{s}'_n) . \tag{42}$$

This identity follows directly from the diagrammatic

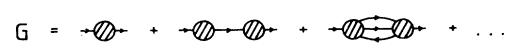

FIG. 11. Renormalized expansion for the one-particle Green's function.

rules for Φ and S_n.

The vertex renormalization described in this section enables one to set up self-consistent approximations beyond finite-order perturbation theory.[24] This will be the subject of a subsequent publication.

IV. LIMIT OF HIGH LATTICE DIMENSION

Recently, the limit of high spatial dimension $d \to \infty$ has been introduced as a new promising starting point for a better understanding of correlated lattice fermions.[15] To obtain nontrivial infinite-dimensional models, the parameters of the nonlocal parts of the Hamiltonian must be properly scaled to compensate (but not overcompensate) for the increase in the number of neighbors on the lattice in high dimensions. For example, the next-neighbor hopping amplitude t must be scaled as

$$t = t^*/(2d)^{1/2}, \quad t^* \text{ fixed} \tag{43}$$

to keep the kinetic energy finite in $d \to \infty$ dimensions.[15]

The limit $d \to \infty$ has been studied for several fermionic lattice models by various approaches,[16] such as perturbation theory with respect to the interaction,[15,25] variational methods,[15,26] and path integral techniques.[27] Exact solutions have been obtained only for a simplified version of the Hubbard model, where only one of the two spin species can hop.[28] The overall conclusions to be drawn from these investigations are

(i) Fermionic lattice models in $d \to \infty$ share many aspects with the corresponding finite-dimensional models—in particular, the dynamical correlations survive in high dimensions; many quantities agree even quantitatively in $d = 3$ and $d = \infty$.

(ii) There are drastic simplifications in $d \to \infty$ which enable one to perform approximate calculations which are prohibitively difficult in finite dimensions, such as, for example, self-consistent perturbation expansions.

(iii) Exact solutions of fermionic lattice models are hard to obtain even in $d \to \infty$ dimensions; standard mean-field theories (with static mean fields) are not exact in this limit.

We will now investigate the perturbation expansion around the atomic limit of the Hubbard model in $d \to \infty$ dimensions. The hopping expansion yields a particularly suggestive real-space picture of the dynamics of lattice fermions in high dimensions.

A. Classification of contributions by powers of $1/d$

The contributions obtained from a perturbation expansion around the atomic limit can be classified by powers of the inverse dimension $1/d$. To be explicit, we restrict the discussion to the case of next-neighbor hopping on a simple hypercubic lattice; generalizations are straightforward. The evaluation of a diagram contributing to the perturbation expansion involves lattice sums which amount to counting the number of possible embeddings of the diagram on the lattice. Each embedding has a certain topology defined by the number of sites "occupied" by the vertices and by the way these sites are connected by the lines of the diagram. In general, the topology of a diagram differs from the topologies of its possible embeddings since different vertices may coincide on one lattice site. In the following the term "topology" refers to the topology of an embedding.

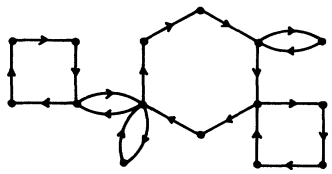

FIG. 12. Topology contributing to Ω in $d = \infty$ dimensions.

We begin by considering the expansion of the grand-canonical potential Ω, where only closed diagrams (without external vertices) are involved (see Rule 1 in Sec. II). In this case only fully two-particle reducible topologies, i.e., topologies constructed by linking polygons (see Fig. 12), survive in the limit $d \to \infty$. This can be seen as follows. A p-gon (having p lines) can extend in up to $p/2$ different spatial dimensions; an embedding consisting of m polygons having $p_1, \ldots, p_m$ lines, respectively, can extend in maximally $p/2$, $p = p_1 + \cdots + p_m$, spatial dimensions, which can be chosen arbitrarily from the d dimensions available on the underlying lattice. For $d \geq p/2$ there are

$$\begin{pmatrix} d \\ p/2 \end{pmatrix}$$

different choices, which is of order $d^{p/2}$ for $d \gg p/2$. Hence, the number of embeddings of a polygon cluster with p lines is of order $d^{p/2}$ for large d. Since each line corresponds to a hopping amplitude $t = t^*/(2d)^{1/2}$, the contribution of such a topology is of order 1.

It is easy to see that topologies which are not fully two-particle reducible are suppressed by some power of $1/d$ as $d \to \infty$. A typical example is given in Fig. 13(a): Each line yields a factor $t^*/(2d)^{1/2}$ whereas the number of embeddings with this topology is only $2d$ (the number of next neighbors on a d-dimensional hypercubic lattice). Hence, this topology is of order $1/d$. The topology shown in Fig. 13(b) is of order $(1/d)^2$ because it contains eight lines while the number of its possible embeddings is of order d^2 for high d.

In $d \to \infty$, many diagrams vanish all together because none of their embeddings have a fully two-particle reduc-

FIG. 13. Topologies of order (a) $1/d$ and (b) $1/d^2$.

ible topology. This is the case, in particular, for the diagram and topology shown in Fig. 13(a). An important dynamical process described by this diagram is the spin exchange where two initially singly occupied sites with different spins exchange their spins (by two hopping processes) and then restore the initial situation (by two other hopping processes). The intermediate spin-exchanged state has zero excitation energy, since the number of doubly occupied sites remains unchanged. This spin-exchange process is the reason why the ground state of the half-filled Hubbard model for a small but finite hopping amplitude is not the Néel state in finite dimensions. In the limit $d \to \infty$, however, this process is suppressed and the Néel state becomes the exact ground state for small hopping amplitude.

The topologies contributing to the Green's functions in high dimensions are also exactly the fully two-particle reducible ones. For the one-particle Green's function $G_{\sigma \mathbf{j}\mathbf{j}'}(\tau,\tau')$ these topologies are chains (running from $\mathbf{j}'$ to $\mathbf{j}$) which may be decorated by local insertions of polygon clusters (see Fig. 14). The contribution of each such topology is proportional to $d^{-s(\mathbf{j},\mathbf{j}')/2}$ where $s(\mathbf{j},\mathbf{j}')$ is the number of next-neighbor steps separating the fixed sites $\mathbf{j}$ and $\mathbf{j}'$ on the lattice. This is easily shown by starting with chains with exactly $s(\mathbf{j},\mathbf{j}')$ lines and by studying the effect of adding further links and local polygon insertions. Topologies containing two-particle irreducible parts are suppressed by some integer power of $1/d$ with respect to the fully reducible ones.

The above discussion implies that

$$G_{\sigma \mathbf{j}\mathbf{j}'}(\tau,\tau') \propto d^{-s(\mathbf{j},\mathbf{j}')/2} \quad \text{as } d \to \infty \ . \tag{44}$$

This result does *not* mean that the off-diagonal elements of G can be neglected in $d \to \infty$, as is shown by the following example. To calculate the kinetic energy

$$E_{\text{kin}} = \sum_{\mathbf{j}\mathbf{j}',\sigma} t_{\mathbf{j}'\mathbf{j}} G_{\sigma \mathbf{j}\mathbf{j}'}(\tau,\tau+0) \tag{45}$$

from the Green's function, one has to sum over many off-diagonal elements of G. For example, each term of the sum corresponding to next neighbors $\mathbf{j}$ and $\mathbf{j}'$ is of order $(1/d^{1/2})^2 = 1/d$ (one factor is due to G, the other to the hopping matrix in (45)]. Since there are $2d$ next neighbors $\mathbf{j}'$ of $\mathbf{j}$, their summed contribution to E_{kin} remains finite as $d \to \infty$.

The topologies contributing to the two-particle cumulants C_2 in $d \to \infty$ dimensions are particle-particle or particle-hole bubble chains which split into two chains at each of their ends; any vertex may be decorated by polygon insertions. A generic example is given in Fig. 15. As in the case of G, the off-diagonal elements of C_2 are suppressed by some power of $1/d$ in $d \to \infty$ dimensions, but partial sums of them (e.g., over all next neighbors) may be finite and can be compared with corresponding results obtained for $d < \infty$.[29]

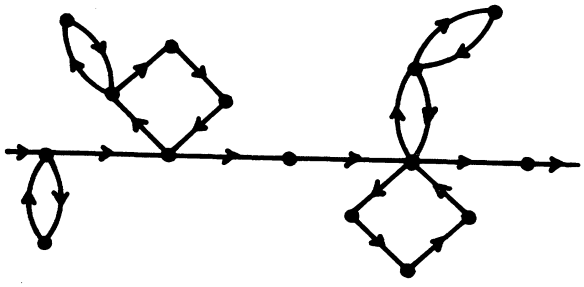

FIG. 14. A typical topology contributing to G in $d = \infty$ dimensions.

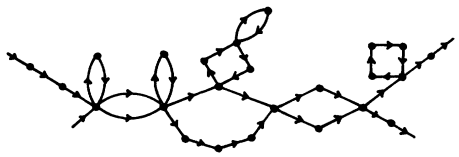

FIG. 15. A typical topology contributing to C_2 in $d = \infty$ dimensions.

B. Dressed-atom picture

We have just shown that in high dimensions the contributing hopping processes are such that the "track" left by the hopping fermions on the lattice is fully two-particle reducible. This result does not hinge upon the particular properties of the linked-cluster expansion: It is valid for any expansion in powers of the hopping matrix. The tracks contributing to the one-particle Green's function have been shown to be chains (with hopping matrix elements as links) which may be decorated by local insertions of polygon clusters. Hence, G has the form (in frequency representation)

$$\begin{aligned} G_{\sigma \mathbf{j}\mathbf{j}'}(\omega) = {} & \delta_{\mathbf{j}\mathbf{j}'} C^{\text{eff}}_{1\mathbf{j}}(\omega\sigma|\omega\sigma) \\ & + C^{\text{eff}}_{1\mathbf{j}}(\omega\sigma|\omega\sigma) t_{\mathbf{j}\mathbf{j}'} C^{\text{eff}}_{1\mathbf{j}'}(\omega\sigma|\omega\sigma) \\ & + \sum_{\mathbf{j}_1} C^{\text{eff}}_{1\mathbf{j}}(\omega\sigma|\omega\sigma) t_{\mathbf{j}\mathbf{j}_1} C^{\text{eff}}_{1\mathbf{j}_1}(\omega\sigma|\omega\sigma) t_{\mathbf{j}_1\mathbf{j}'} \\ & \times C^{\text{eff}}_{1\mathbf{j}'}(\omega\sigma|\omega\sigma) + \cdots \ . \end{aligned} \tag{46}$$

where C^{eff}_1 is given by the bare atomic one-particle cumulant C^0_1 plus all local decorations. From (46) one obtains a Dyson-type equation relating G and C^{eff}_1:

$$\begin{aligned} G_{\sigma \mathbf{j}\mathbf{j}'}(\omega) = {} & \delta_{\mathbf{j}\mathbf{j}'} C^{\text{eff}}_{1\mathbf{j}}(\omega\sigma|\omega\sigma) \\ & + \sum_{\mathbf{j}_1} C^{\text{eff}}_{1\mathbf{j}}(\omega\sigma|\omega\sigma) t_{\mathbf{j}\mathbf{j}_1} G_{\sigma \mathbf{j}_1\mathbf{j}'}(\omega) \ . \end{aligned} \tag{47}$$

The chain structure (46) of G has an interesting implication: the single-particle properties of locally interacting tight-binding fermions in high dimensions are the same as those of *independent* tight-binding fermions hopping between "*dressed*" *atoms* with a certain internal structure characterized by an effective atomic Green's function C^{eff}_1. By comparing (47) with the usual Dyson equation $G = G_0 + G_0 \Sigma G$, where Σ is the self-energy and $G_0 = (i\omega + \mu - t)^{-1}$ the one-particle Green's function for $U = 0$ (t is the hopping matrix), one finds that Σ is a local (site-diagonal) function given by

$$\Sigma_{\sigma jj'}(\omega)=\begin{cases} i\omega+\mu-[C^{\rm eff}_{1j}(\omega\sigma|\omega\sigma)]^{-1} & \text{for } j=j' , \\ 0 \quad \text{for } j\neq j' . \end{cases} \tag{48}$$

The result that the self-energy is local in $d=\infty$ has already been obtained earlier within perturbation theory with respect to the Hubbard interaction U.[25] Since the same result has now been obtained within perturbation theory around the atomic limit, it is highly plausible that the *exact* self-energy also becomes local in the limit $d\rightarrow\infty$,

C. Half-filled band at zero temperature

For the special case of a half-filled band ($n_\uparrow+n_\downarrow=1$) in $d=\infty$ dimensions it is possible to perform a ground-state perturbation expansion around the atomic limit. In general, this is prohibited by the (infinite-dimensional) degeneracy of the ground state of H_0 (1b); degenerate perturbation theory around H_0 involves exact solutions of effective Hamiltonians, which are not much simpler than the Hubbard model itself. For the half-filled-band case the effective Hamiltonian ensuing from degenerate perturbation theory is the Heisenberg model

$$H_J=\sum_{i,j} J_{ij}\vec{S}_i\cdot\vec{S}_j , \tag{49}$$

where $J_{ij}=4t_{ij}^2/U$.[30] The degeneracy is lifted by H_J (the ground state of H_J is unique up to global symmetries). The explicit evaluation of the perturbation expansion around the atomic limit involves the calculation of correlation functions for the ground state of H_J.[31] This is not possible in general. In high dimensions, however, the ground state of the Heisenberg Hamiltonian H_J is given exactly by the mean-field result.[32] On a hypercubic lattice the mean-field ground state of H_J is the Néel state (provided that next-neighbor hopping is the dominant hopping amplitude in t_{ij}). Hence, the Néel state is the exact ground state for the half-filled Hubbard model with infinitesimally small t_{ij}/U and higher orders (in t_{ij}/U) can be calculated by expanding around the Néel state.

The diagrammatic rules for the evaluation of the ground-state energy and the Green's functions can be obtained from the finite-temperature rules (rules 1, 2, and 3 in Sec. II) by (i) taking the limit $T\rightarrow 0$, (ii) analytically continuing the imaginary times τ to real times t, and (iii) inserting the Néel state cumulants for C^0_m. Thus, Rules 1, 2, and 3 in Sec. II are only slightly modified: the lines are now labeled by real-time variables (instead of imaginary-time variables) which are integrated from $-\infty$ to ∞ (instead of from 0 to β); the vertices correspond to cumulants

$$C^0_{mj}(t_1\sigma_1,\ldots,t_m\sigma_m|t'_1\sigma'_1,\ldots,t'_m\sigma'_m) ,$$

which are calculated from the atomic zero-temperature Green's functions

$$G^0_{nj}(t_1\sigma_1,\ldots,t_n\sigma_n|t'_1\sigma'_1,\ldots,t'_n\sigma'_n)=(-i)^n\langle\Phi_0|\mathcal{T}[\hat{c}_{j\sigma_1}(t_1)\ldots\hat{c}_{j\sigma_n}(t_n)\hat{c}^\dagger_{j\sigma'_n}(t'_n)\ldots\hat{c}^\dagger_{j\sigma'_1}(t'_1)]\Phi_0\rangle \tag{50}$$

by using the cumulant decomposition of G^0_n (see Sec. II). Here $|\Phi_0\rangle$ is the Néel state

$$|\Phi_0\rangle=\left[\prod_{j\in A} c^\dagger_{j\uparrow}\right]\left[\prod_{j\in B} c^\dagger_{j\downarrow}\right]|0\rangle \tag{51}$$

created by filling the A sublattice with up spins and the B sublattice with down spins. The time dependence of the operators in (50) is given by

$$\hat{c}_{j\sigma}(t)=e^{i\hat{H}_0 t}c_{j\sigma}e^{-i\hat{H}_0 t} , \tag{52a}$$

$$\hat{c}^\dagger_{j\sigma}(t)=e^{i\hat{H}_0 t}c^\dagger_{j\sigma}e^{-i\hat{H}_0 t} . \tag{52b}$$

In this way the atomic one-particle cumulant is obtained as

$$C^0_{1j}(t\sigma|t'\sigma')=\begin{cases} i\delta_{\sigma\sigma'}\Theta(t'-t) & \text{if j is on } X_\sigma \\ -i\delta_{\sigma\sigma'}\Theta(t-t')e^{-iU(t-t')} & \\ \qquad\qquad \text{if j is on } X_{-\sigma} , & \end{cases} \tag{53}$$

where X_σ is the sublattice occupied by a σ spin in the Néel state $|\Phi_0\rangle$, i.e., $X_\uparrow=A$, $X_\downarrow=B$.

The frequency representation of C^0_1 reads

$$C^0_{1j}(\omega\sigma|\omega\sigma')=\begin{cases} \delta_{\sigma\sigma'}/(\omega-i\eta) & \text{if j is on } X_\sigma \\ \delta_{\sigma\sigma'}/(\omega-U+i\eta) & \text{if j is on } X_{-\sigma} , \end{cases} \tag{54}$$

where η is an infinitesimally small positive number enforcing convergence of the Fourier transformations. The atomic two-particle cumulant is nonzero only if $\sigma_1=-\sigma_2$ and $\sigma'_1=-\sigma'_2$; in this case it is given by

$$C^0_{2j}(\omega_1+\omega,\sigma,\omega_2-\omega,-\sigma|\omega_1,\sigma,\omega_2,-\sigma)$$
$$=i\frac{1}{\omega_1+\omega-i\eta}\frac{1}{\omega_2-\omega-U+i\eta}\frac{1}{\omega_1-i\eta}\frac{1}{\omega_2-U+i\eta}$$
$$\times\left[U+\frac{U^2}{\omega_1-\omega_2+\omega-i\eta}\right] \quad \text{for j on } X_\sigma . \tag{55}$$

For j on $X_{-\sigma}$ one has $\omega_1\leftrightarrow\omega_2$ and $\omega\leftrightarrow-\omega$ in (55). Note that the first four factors on the right-hand side (r.h.s) of (55) are just the one-particle cumulants C^0_1 of the two entering and the two leaving particles, respectively.

We conclude this section by listing the results which have been obtained by explicit evaluation of diagrams up to a certain order. All time and frequency integrals are elementary, i.e., each diagram can be calculated analytically. All quantities are calculated for next-neighbor hopping with an amplitude

$$t_{ij}=-t=-t^*/(2d)^{1/2}$$

on a hypercubic lattice. The results are exact (to a certain order in t^*/U) only in $d\rightarrow\infty$ dimensions, but they may be used as in approximation for three-dimensional itinerant antiferromagnets in the strong-correlation regime ($U\gg t$).

The one-particle zero-temperature Green's function is defined by

$$G_{\sigma \mathbf{j}\mathbf{j}'}(t,t') = -i\langle \Psi_0 | \mathcal{T}[\tilde{c}_{\mathbf{j}\sigma}(t)\tilde{c}^{\dagger}_{\mathbf{j}'\sigma}(t')] | \Psi_0 \rangle \ , \tag{56}$$

where $|\Psi_0\rangle$ is the exact ground state of the Hubbard model H (1a)–(1c), and $\tilde{c}^{\dagger}, \tilde{c}$ are creation and annihilation operators in Heisenberg representation with respect to H. The Green's function has been calculated up to third order in t^*/U. The results are listed in Appendix B.

The one-particle density matrix

$$P_{\sigma \mathbf{i}\mathbf{j}} = \langle \Psi_0 | c^{\dagger}_{\mathbf{i}\sigma} c_{\mathbf{j}\sigma} | \Psi_0 \rangle \tag{57}$$

can be calculated from the Green's function. The nth-order contributions $P^n_{\sigma \mathbf{i}\mathbf{j}}$ are (for $n = 0,1,2,3$)

$$P^0_{\sigma \mathbf{i}\mathbf{j}} = \delta_{\mathbf{i}\mathbf{j}}\delta_{\mathbf{i}\sigma} \ , \tag{58a}$$

$$P^1_{\sigma \mathbf{i}\mathbf{j}} = \frac{t}{U} p^1_{\mathbf{i}\mathbf{j}} \ , \tag{58b}$$

$$P^2_{\sigma \mathbf{i}\mathbf{j}} = \frac{t^2}{U^2} p^2_{\mathbf{i}\mathbf{j}} (-\delta_{\mathbf{i}\sigma} + \delta_{\mathbf{i}-\sigma}) \ , \tag{58c}$$

$$P^3_{\sigma \mathbf{i}\mathbf{j}} = \frac{t^3}{U^3} (-2p^3_{\mathbf{i}\mathbf{j}} + 4p^2_{\mathbf{i}\mathbf{i}} p^1_{\mathbf{i}\mathbf{j}}) \ , \tag{58d}$$

where $p^n_{\mathbf{i}\mathbf{j}}$ is the number of different lattice walks leading from $\mathbf{i}$ to $\mathbf{j}$ after n next-neighbor steps ($p^1_{\mathbf{i}\mathbf{j}} = 1$ if $\mathbf{i},\mathbf{j}$ are next neighbors, 0 otherwise; $p^2_{\mathbf{i}\mathbf{i}} = 2d$; $p^3_{\mathbf{i}\mathbf{j}} = 6d - 3$ if $\mathbf{i},\mathbf{j}$ are next neighbors, etc.). For the sublattice magnetization

$$m \equiv |\langle \Psi_0 | n_{\mathbf{j}\sigma} - n_{\mathbf{j},-\sigma} | \Psi_0 \rangle| \ , \tag{59}$$

one obtains

$$m = 1 - 2(t^*/U)^2 + O((t^*/U)^4) \ . \tag{60}$$

The ground-state energy E has been calculated up to fifth order in t^*/U. It is given by

$$E/L = -t^{*2}/U + t^{*4}/U^3 + O(t^{*6}/U^5) \ , \tag{61}$$

where L is the number of lattice sites. It is interesting to note that the antiferromagnetic Hartree-Fock solution yields

$$E/L = -t^{*2}/U + 2t^{*4}/U^3 + O(t^{*6}/U^5) \ ,$$

while the antiferromagnetic Gutzwiller wave function yields

$$E/L = -t^{*2}/U + t^{*4}/U^3 + O(t^{*6}/U^5)$$

(Ref. 33), which is exact up to order t^{*5}/U^4.

V. CONCLUSIONS

A finite-temperature perturbation expansion around the atomic limit of the Hubbard model has been developed. The unrenormalized expansion has been formulated in terms of simple diagrammatic rules for the calculation of the grand-canonical potential Ω and of n-particle Green's functions G_n in powers of the hopping amplitude. Discrepancies in earlier expansions[8–12] around the atomic limit have been clarified in favor of works by Kubo[8] and Kubo and Tada[11] by calculating finite-order contributions to the grand-canonical potential and by comparing with a corresponding exact result in one dimension.

The diagrammatic rules reduce the calculation of finite-order contributions to Ω or G_n to simple algebra, which becomes, however, increasingly cumbersome for higher orders. Fortunately, any step of the rules can be carried out exactly by a computer program (even the time integrals and/or frequency sums, because they are all of the same type). Hence, one will be able to go to relatively high orders, such that the method of series extrapolation, which has been very successful for spin models, can be applied.

In contrast to previous approaches, the expansion discussed in this paper involves only *connected* diagrams with *unrestricted* lattice sums. This made possible a vertex renormalization analogous to the renormalization known for the linked-cluster expansion of the Ising model.[4] The renormalized perturbation expansion provides a basis for the construction of self-consistent approximations, where Green's functions are obtained by functionally differentiating a generating functional Φ with respect to external, time-dependent fields. In contrast to the well-known self-consistent expansions around the noninteracting Fermi sea, in our approach the atomic limit is automatically treated exactly. To describe the noninteracting limit $U \to 0$ exactly, too, it is sufficient to include all diagrams consisting exclusively of one-particle vertices, because higher-order vertices vanish for $U \to 0$. In particular, for the one-particle Green's function these are just the chain diagrams.

The hopping expansion is particularly suitable for visualizing the peculiarities of special lattice structures. It was shown that for a high-dimensional ($d \to \infty$) lattice only fully two-particle reducible embeddings of diagrams contribute. As a consequence, the single-particle properties of locally interacting fermions in $d \to \infty$ dimensions were seen to reduce to those of independent tight-binding fermions hopping between dressed atoms. The self-energy was shown to be local in $d \to \infty$ dimensions [this property had so far been derived only within perturbation theory with respect to U (Ref. 25)].

The technique developed in this work can be easily generalized for any lattice model of the form $H = H_0 + H_1$, where H_0 is a sum of local operators and H_1 is a sum of arbitrary two-fermion operators. Thereby, the diagrammatic rules remain essentially unchanged. A generalization of H_0 (e.g., to a many-orbital atom) affects only the atomic cumulants C^0_m (corresponding to the vertices of a diagram). A generalized H_1 (including interband transitions, spin-dependent hopping amplitudes, etc.) leads to generalized hopping matrices $t^{\alpha\beta}_{\mathbf{i}\mathbf{j}}$ (corresponding to the lines of a diagram), where α,β are band or spin indices.

ACKNOWLEDGMENTS

I am grateful to Professor D. Vollhardt for useful discussions and for a critical reading of the manuscript. I

have also profitted from conversations with Professor G. Czycholl, Dr. P. van Dongen, and Dr. F. Gebhard. This work was supported in part by the Studienstiftung des Deutschen Volkes and by the Sonderforschungsbereich 341 of the Deutsche Forschungsgemeinschaft.

APPENDIX A: RELATION BETWEEN Ω AND Φ

Equation (41) relating Ω and Φ is easily proven by introducing time- and spin-dependent hopping matrix elements $t_{ij}(s';s)$. The S matrix (5) involved in the interaction representation (4) of Ω is then generalized to

$$\hat{S}=\mathcal{T}\exp\left[-\int_0^\beta d\tau\, d\tau' \sum_{\sigma,\sigma'}\sum_{j,j'} t_{j'j}(\tau'\sigma';\tau\sigma)\hat{c}^\dagger_{j'\sigma'}(\tau')\hat{c}_{j\sigma}(\tau)\right] . \tag{A1}$$

Clearly, the only modification in the diagrammatic rules caused by this generalization is that the lines become time-and spin-dependent functions $t_{j'j}(s';s)$. Comparing the interaction representation for Ω (4), with the one for G (26), one finds that

$$\frac{\delta\Omega}{\delta t_{j'j}(s';s)}=G_{jj'}(s|s') , \tag{A2}$$

where $G_{jj'}(s|s')$ is the exact one-particle Green's function in the presence of the generalized hopping matrices.

We now show that the functional derivative of the r.h.s. of (41) with respect to $t_{j'j}(s';s)$ also yields $G_{jj'}(s|s')$. The functional Ω (defined by its expansion) depends on t explicitly (via the lines) and implicitly (via the renormalized vertices). Hence, we obtain

$$\begin{aligned}\frac{\delta\Phi}{\delta t_{j'j}(s';s)}&=\left[\frac{\delta\Phi}{\delta t_{j'j}(s';s)}\right]_{\bar{C}}+\sum_{n=1}^{\infty}\sum_i\int d\vec{s}_n d\vec{s}\,'_n\frac{\delta\Phi}{\delta\bar{C}_{ni}(\vec{s}_n|\vec{s}\,'_n)}\frac{\delta\bar{C}_{ni}(\vec{s}_n|\vec{s}\,'_n)}{\delta t_{j'j}(s';s)}\\&=G_{jj'}(s|s')+\sum_{n=1}^{\infty}\sum_i\int d\vec{s}_n d\vec{s}\,'_n S_{ni}(\vec{s}_n|\vec{s}\,'_n)\frac{\delta\bar{C}_{ni}(\vec{s}_n|\vec{s}\,'_n)}{\delta t_{j'j}(s';s)} ,\end{aligned} \tag{A3}$$

where the last step follows from the fact that functional derivation of Ω with respect to the hopping matrix (for fixed $\bar{C}_m$, $m=1,2,\ldots$) corresponds to breaking lines in the diagrams (first term) and from (42) (second term). The renormalized zero-particle cumulant $\bar{C}_{0j}$, defined by (38), depends on $t_{j'j}(s';s)$ only via the self-fields. Hence,

$$\begin{aligned}\sum_i\frac{\delta\bar{C}_{0i}}{\delta t_{j'j}(s';s)}&=\sum_i\sum_{n=1}^{\infty}\int d\vec{s}_n d\vec{s}\,'_n\frac{\delta\bar{C}_{0i}}{\delta S_{ni}(\vec{s}_n|\vec{s}\,'_n)}\frac{\delta S_{ni}(\vec{s}_n|\vec{s}\,'_n)}{\delta t_{j'j}(s';s)}\\&=\sum_i\sum_{n=1}^{\infty}\int d\vec{s}_n d\vec{s}\,'_n\bar{C}_{ni}(\vec{s}_n|\vec{s}\,'_n)\frac{\delta S_{ni}(\vec{s}_n|\vec{s}\,'_n)}{\delta t_{j'j}(s';s)} ,\end{aligned} \tag{A4}$$

where in the last step the identity (39) has been applied. Using (A3) and (A4), we find that the functional derivative of the rhs of (41) with respect to $t_{j'j}(s';s)$ yields indeed the exact Green's function $G_{jj'}(s|s')$. Since (41) is trivially satisfied for $t_{j'j}(s',s)=0$ (in this case $\Omega=\Omega_0$, $\Phi=0$, $S_n=0$, $\bar{C}_n=C_n^0$), the equality for the derivatives implies that (41) holds for arbitrary $t_{j'j}(s',s)$ and, in particular, for the "static" hopping matrix

$$t_{j'j}(s';s)=\delta_{\sigma\sigma'}\delta(\tau-\tau')t_{j'j} ,$$

Q.E.D.

APPENDIX B: GROUND-STATE GREEN'S FUNCTION FOR THE HALF-FILLED STRONGLY COUPLED HUBBARD MODEL IN $d=\infty$ DIMENSION

For the ground state of the half-filled Hubbard model on an infinite-dimensional lattice with next-neighbor hopping (amplitude $-t$), the leading corrections to the atomic Green's function (Néel-state Greens function) are given by

$$G^1_{\sigma jj'}(\omega)=-tp^1_{jj'}\frac{1}{\omega-i\eta}\frac{1}{\omega-U+i\eta} , \tag{B1}$$

$$G^2=G^{2a}+G^{2b} , \tag{B2}$$

where

$$G^{2a}_{\sigma jj'}(\omega)=t^2 p^2_{jj'}\frac{1}{\omega-i\eta}\frac{1}{\omega-U+i\eta}\left[\frac{\delta_{j\sigma}}{\omega-i\eta}+\frac{\delta_{j,-\sigma}}{\omega-U+i\eta}\right]$$

$$G^{2b}_{\sigma jj'}(\omega)=\delta_{jj'}t^2 p^2_{jj}\frac{\delta_{j\sigma}}{(\omega-i\eta)^2}\left[\frac{1}{U}+\frac{1}{\omega-i\eta}\right]+\delta_{jj'}t^2 p^2_{jj}\frac{\delta_{j,-\sigma}}{(\omega-U+i\eta)^2}\left[-\frac{1}{U}+\frac{1}{\omega-U+i\eta}\right], \tag{B3}$$

$$G^3=G^{3a}+G^{3b}+G^{3c},$$

where

$$G^{3a}_{\sigma jj'}(\omega)=-t^3 p^3_{jj'}\frac{1}{(\omega-i\eta)^2}\frac{1}{(\omega-U+i\eta)^2},$$

$$G^{3b}_{\sigma jj'}(\omega)=-t^3 p^2_{jj}p^1_{jj'}\left[\delta_{j'\sigma}\left[\frac{1}{U}+\frac{1}{\omega-i\eta}\right]\frac{1}{(\omega-i\eta)^2}\frac{1}{\omega-U+i\eta}+\delta_{j',-\sigma}\left[-\frac{1}{U}+\frac{1}{\omega-U+i\eta}\right]\frac{1}{(\omega-U+i\eta)^2}\frac{1}{\omega-i\eta}\right],$$

$$G^{3c}_{\sigma jj'}(\omega)=G^{3b}_{\sigma j'j}(\omega).$$

Here $\delta_{j\sigma}=1$ if j belongs to X_σ [the sublattice filled with σ spins in $|\Phi_0\rangle$ (51)] and $\delta_{j\sigma}=0$ otherwise; $p^n_{jj'}$ is the number of possible n-step lattice walks from j to j'.

---

*Present address: Dipartimento di Fisica, c/o Professor C. Di Castro, Università "La Sapienza," 00185 Roma, Italy.

[1]For a theoretical review, see T. M. Rice, Z. Phys. B **67**, 141 (1987); A. S. Davidov, Phys. Rep. **190**, 191 (1990).

[2]For reviews on series expansions, see *Phase Transitions and Critical Phenomena,* edited by C. Domb and M. S. Green (Academic, London, 1974), Vol. 3.

[3]See, for example, the article by D. D. Betts in Ref. 2.

[4]For a review, see M. Wortis in Ref. 2.

[5]M. C. Gutzwiller, Phys. Rev. Lett. **10**, 159 (1963).

[6]J. Hubbard, Proc. R. Soc. London, Ser. A **276**, 238 (1963).

[7]J. Kanamori, Prog. Theor. Phys. **30**, 275 (1963).

[8]K. Kubo, Prog. Theor. Phys. **64**, 758 (1990).

[9]G. Beni, P. Pincus, and D. Hone, Phys. Rev. B **8**, 3389 (1973).

[10]B. H. Zhao, H. Q. Nie, K. Y. Zhang, K. A. Chao, and R. Micnas, Phys. Rev. B **36**, 2321 (1987).

[11]K. Kubo and M. Tada, Progr. Theor. Phys. **69**, 1345 (1983); **71**, 479 (1984).

[12]M. Plischke, J. Stat. Phys. **11**, 159 (1974).

[13]J. Hubbard, Proc. R. Soc. London, Ser. A **296**, 82 (1966).

[14]See, for example, S. Schmitt-Rink and A. E. Ruckenstein, Phys. Rev. B **38**, 7188 (1988).

[15]W. Metzner and D. Vollhardt, Phys. Rev. Lett. **62**, 324 (1989).

[16]For a review, see D. Vollhardt, Int. J. Mod. Phys. B **3**, 2189 (1989); E. Müller-Hartmann, *ibid.* **3**, 2169 (1989); W. Metzner and D. Vollhardt, Helv. Phys. Acta **63**, 364 (1990).

[17]Note that here the kinetic energy H_1 plays the role of the "interaction."

[18]See, for example, J. W. Negele and H. Orland, *Quantum Many-Particle Systems* (Addison-Wesley, New York, 1988), Chap. 2.

[19]A clear proof of the linked-cluster theorem for an analogous expansion of the Ising model is given in Ref. 4; the proof also applies to the present expansion of the Hubbard model.

[20]J. L. Martin in Ref. 2.

[21]J. B. Sokoloff, Phys. Rev. B **2**, 779 (1970); G. Beni, T. Holstein, and P. Pincus, *ibid.* **8**, 312 (1973).

[22]For a review, see D. S. Gaunt and A. J. Guttmann in Ref. 2.

[23]The only attempts known to the author have been made in Refs. 11 and 12 for the special case $U=\infty$.

[24]Examples for such self-consistent approximations derived from the analogous linked-cluster expansion of the Ising model are described in Ref. 4.

[25]E. Müller-Hartmann, Z. Phys. B **74**, 507 (1989); **76**, 211 (1989); H. Schweitzer and G. Czycholl, Solid State Commun. **69**, 171 (1989); (unpublished).

[26]P. G. J. van Dongen, F. Gebhard, and D. Vollhardt, Z. Phys. B **76**, 199 (1989); W. Metzner, *ibid.* **77**, 253 (1989); P. Fazekas, B. Menge, and E. Müller-Hartmann, *ibid.* **78**, 69 (1990); F. Gebhard, Phys. Rev. B **41**, 9452 (1990).

[27]V. Janis (unpublished); H. Hasegawa (unpublished).

[28]U. Brandt and C. Mielsch, Z. Phys. B **75**, 365 (1989); **79**, 295 (1990); P. G. J. van Dongen and D. Vollhardt, Phys. Rev. Lett. **65**, 1663 (1990).

[29]The spatial structure of correlation functions within correlated variational wave functions in $d\rightarrow\infty$ dimensions has already been clarified by P. G. J. van Dongen, F. Gebhard, and D. Vollhardt in Ref. 26.

[30]P. W. Anderson, in *Solid State Physics* (Academic, New York, 1963), Vol. 14, p. 99.

[31]M. Takahashi, J. Phys. C **10**, 1289 (1977).

[32]T. Kennedy, E. H. Lieb, and B. S. Shastry, Phys. Rev. Lett. **61**, 2582 (1988).

[33]P. Fazekas, B. Menge, and E. Müller-Hartmann in Ref. 26.